Predominant transport paths of Saharan dust over the Mediterranean Sea to Europe

P. Israelevich, E. Ganor, P. Alpert, P. Kishcha and A. Stupp

Department of Geophysics and Planetary Sciences, Tel Aviv University, Tel Aviv, 69978, Israel.

P. Israelevich, E. Ganor, P. Alpert, P. Kishcha, and A. Stupp

P. Alpert, Department of Geophysics and Planetary Sciences, Tel Aviv University, Tel Aviv, 69978, Israel.

E. Ganor, Department of Geophysics and Planetary Sciences, Tel Aviv University, Tel Aviv, 69978, Israel.

P. Israelevich, Department of Geophysics and Planetary Sciences, Tel Aviv University, Tel Aviv, 69978, Israel. (peter@post.tau.ac.il)

P. Kishcha, Department of Geophysics and Planetary Sciences, Tel Aviv University, Tel Aviv, 69978, Israel.

A. Stupp, Department of Geophysics and Planetary Sciences, Tel Aviv University, Tel Aviv, 69978, Israel.

Abstract. We use monthly data of aerosol optical thickness (AOT) from the Moderate Resolution Imaging Spectroradiometer (MODIS) on board the 7 NASA Terra and Aqua satellites for the ten-year period (2001 -2010) in order to determine seasonal variations of Saharan dust transport over the Mediterranean towards Europe. The maxima of AOT are used to visualize the transport paths. Saharan dust reaches Europe over the Mediterranean, and also by looping back over the Atlantic. In spring, aerosols are observed within a wide range of longitudes in Europe, with the highest AOT over West Europe. This may be partially explained by dust transport to Western Europe via the Atlantic route, while to Central and Eastern Europe dust is transported over the Mediterranean. During all seasons dust is transported over the Mediterranean to Europe. In the summer months, aerosols are observed predominantly in Central Europe. In autumn, aerosol activity is strongest in Eastern Europe. We show that there are local AOT maxima over North Italy, in the Alps, in Spain, South-East of the Pyrenees and Sierra Nevada, and in the Rila Mountains in Bulgaria. We suggest that these maxima of aerosol concentration appear as the dust-carrying air flow reaches the mountains and slows.

1. Introduction

The Sahara desert is one of the major producing regions of dust particles affecting the radiative budget in the Earth's atmosphere. Most of the Saharan dust is transported over the Atlantic Ocean toward the Americas by trade winds [*Prospero*, 1999]. However, a significant fraction of the dust load from African sources participates in atmospheric circulation above the Mediterranean Sea and Europe [*Engelstaedter et al*., 2006; *Engelstaedter and Washington*, 2007; *Ganor et al.*, 2000; *Goudie and Middleton*, 2001; *Barkan et al*., 2004a, 2005]. Desert dust aerosol may impact regional climate, the biogeochemical cycle, and human environments (even mortality rate, e.g. [*Sajani et al*., 2010; *Perez et al*., 2008]). The aerosol affects the atmosphere both directly by changing reflection and absorption of the solar radiation and indirectly by influencing cloud albedo, precipitation development and cloud lifetime [*Levin et al*., 1996; *Wurzler et al*., 2000; *Rosenfeld et al.*, 2001; *Yin et al*., 2002].

There are no desert dust sources in Europe, nevertheless, the desert dust was observed, at least occasionally, in different regions of Europe [e.g. *Littman and Steinrucke*, 1989; *Barnaba and Gobbi*, 2004; *Koltay et al.*, 2006; *Perez et al.*, 2008; *Pieri et al.*, 2010; *Sajani et al*., 2010; *Gerasopoulos et al*., 2011]. The events with high aerosol optical thickness (AOT) in this region are associated with biomass burning (not only in Europe, smoke from North America may also reach the continent), anthropogenic pollution, soil erosion, transported dust from Sahara sources and volcanic ash. Except the latter, all of them are expected to reveal seasonal variations [*Escudero et al*., 2005; *Querol et al*., 2009; *Papayannis et al*., 2008].

Desert dust transport in the Mediterranean region exhibits distinct long-term climate-controlled [*Jilbert et al*., 2010] and annual variability [*Moulin et al.*, 1997, 1998; *Barkan et al*., 2004a; *Barnaba and Gobbi*, 2004; *Engelstaedter and Washington*, 2007]. Annual changes are primarily determined by two independent factors: (a) seasonal dependence of dust sources strength in Africa [*Barkan and Alpert, 2008*] and (b) seasonal changes in the atmospheric circulation [*Israelevich et al., 2002*]. Comprehensive statistical study of dust episodes [*Ganor et al.*, 2010; *Gkikas et al*., 2009] reveals a clear difference between Eastern and Western Mediterranean in aerosol activity and its seasonal dependence. The dynamics of individual aerosol event can be followed using satellite observations (TOMS, MODIS) or model simulations (e.g. DREAM) thus revealing aerosol trajectories for the 55 specific case [*Kishcha et al*., 2008]. In spring and summer the air over North Africa is almost permanently loaded with significant amounts of dust. This dust is mobilized and transported northwards and eastwards along the Mediterranean coast [Ganor et al., 2010]. For the eastern Mediterranean the three periods of increased atmospheric dust are in spring (March-May), in summer (July-August) and in autumn (September-November) [*Israelevich et al*., 2003]. Aerosol vertical distribution exhibits different behavior during these periods [*Kalivitis et al.*, 2007]. There is a distinct difference in the particle size distributions and the real and imaginary parts of the refractive indices for these periods indicating that different dust sources play major role during different seasons [*Israelevich et al*., 2003].

Each case of desert dust presence in Europe is associated with a certain trajectory of dust loaded airmass. These individual trajectories differ significantly from event to event. The primary goal of this study is to determine (1) whether there are predominant transport paths by which the dust from North Africa reaches Europe, and (2) do these paths, if exist, exhibit seasonal variations. The transport paths or routes considered in this study are not trajectories, but rather regions where the trajectories occur with highest probability. AOT maxima are used to visualize the aerosol transport route. In accordance with the continuity equation, local maxima of averaged over long time period AOT appear either above the aerosol source or in the region where the divergence of horizontal aerosol containing flow has minimum [*Israelevich et al*., 2002], whereas the band of increased average AOT visualizes the typical aerosol transport route during the period of averaging. Obviously, the direction of aerosol propagation is opposite to the AOT gradient, i.e. from high to low AOT values. The study is carried out by analyzing 10-year mean distributions of MODIS AOT over the Mediterranean and Europe in different seasons.

2. Data

The idea to use satellite aerosol data in order to investigate major routes of Saharan dust transport towards Europe is illustrated in Fig. 1.

There are two ways for dust from Africa to reach Western Europe. A dust plume intruding into the Atlantic Ocean may turn to the North and then be swept eastward toward Europe as shown in Fig. 1 (top left panel). Desert aerosol may also move directly into Europe over the Mediterranean (top right panel, Fig. 1). Both transport possibilities occur. Bottom panels in Fig. 1 show the distributions of TOMS aerosol index on March 5, 1997 (Atlantic path, left panel) and on October 12, 2001 (Mediterranean path, right panel). Systematic statistical studies may help to understand which of the two paths is more common in different seasons.

In order to obtain the aerosol transport paths above the region of interest, we analyze 10-year (2001 - 2010) average MODIS AOT distributions. We use daily distributions of mean AOT as observed by the Moderate Resolution Imaging Spectroradiometer (MODIS) [Remer et al., 2005] on the Terra and Aqua satellites at λ = 550 nm from the collection 5 Level- 3 (1° gridded) daytime daily data (datasets MOD08 D3 and MYD08 D3) at the data archive at http://ladsweb.nascom.nasa.gov/data/search.html. Daily distributions of OMI UV Aerosol index from the Version-003 of Level-3 Aura/OMI daily global TOMS-Like Total Column Ozone gridded product (OMTO3d) were also used.

The distributions are provided on a geographical grid with a resolution of 1^o x1^o . The averaged seasonal distributions were calculated by averaging individual daily distributions for the period 2001-2010 (January 2001 -December 2010 for the Terra satellite, and July 2002 -December 2010 for the Aqua satellite).

It is worth mentioning, that MODIS AOT data are absent for the regions with high albedo, namely for the Sahara desert with its dust sources and for snow-covered regions in Europe. Furthermore, MODIS AOT data did not allow us to distinguish between different types of aerosol - desert dust, biomass burning products, anthropogenic industrial pollution, agricultural soil erosion, volcanic ash, sea salt aerosols etc. Such an ambiguity is, to some extent, intrinsic for any remote measurements of aerosol, and only mineralogical studies allow exact determination of aerosol type. Nevertheless, if the band of enhanced AOT starts from North Africa, it is very probable that it is the path of desert dust transport. Vice versa, the bands starting in Europe are associated with other types of aerosols.

Although the bands of the enhanced averaged AOT visualize major dust transport routes, long term averaging does not allow us to distinguish individual dust events. Therefore, the attempts to calculate backward trajectories of aerosol motion are superfluous. The same is true for an analysis of meteorological situations. Such an analysis could be helpful

for studying some specific dust events. However, it cannot be applied to a dust pattern averaged over a long period of time. In addition, it should be noted that different meteorological situations may result in the same direction of aerosol transport. For example, both a cyclone westward from the dust source and an anticyclone eastward from the source causes northward dust transport. Hence, the long term average direction of aerosol transport is not necessarily associated with a certain meteorological situation.

3. Strong Dust Events and ”Background” Transport

The necessity of this approach, in particular, is based on the fact that strong events provide significant but not the major part of multi-year mean AOD values. According to *Gkikas et al*. [2009], the number of strong events above the Mediterranean with AOT between <AOT> +2σ and <AOT> +4σ is about 7 episodes per year, and there are about 3 per year extreme events with AOT greater than <AOT> +4σ. Here <AOT> stands for the average AOT and σ stands for the standard deviation. Taking as an estimate σ approximately equal to <AOT> and two days as the duration of an event [*Ganor,* 1994; *Ganor et al*., 2010], one estimate that the total aerosol loading during strong aerosol events as follows: <AOT_STRONG> = (d*N_s*AOT_s+ d*N_e*AOT_e)/365, where d is the duration of event (estimated as 2 days, N is the number of events per year, indices e and s refer to extremely strong events and strong events, respectively. N_e = 3, N_s = 7, AOT*e* is estimated as 5*<AOT>, AOT*s* – as 3*<AOT>. Thus, <AOT_STRONG> = (2*3*7+2*5*3)/365 = 0.2*<AOT>, i.e. only 20% of total aerosol loading is due to the strong and extremely strong events. is about 20% of the total loading. Therefore, the major part (80%) of the aerosol loading is produced by smaller events which may even overlap producing almost continuous loading.

In order to determine the relative role of strong dust events in total aerosol transport more accurately, let us consider the daily AOT integrated over the Mediterranean region (0^o -40^o E, 30^o N -40^o N):

$$B_M(t_i) = \int_{30}^{40}\int_{0}^{40} AOT(t_i, \varphi, \lambda)\, d\varphi\, d\lambda \qquad (1)$$

The time dependence of this measure of the aerosol amount in the atmosphere for 2003 is shown in Fig. 2 (thick solid line). Thin line shows the lower envelope b_M (t) of the curve B_M (t). Whereas the integral of B_M (t)) over the time gives the total amount of aerosol in the atmosphere during the period, the integral of b_M(t) estimates the amount in absence of dust events. The ratio $\int_{year} b_M(t)dt / \int_{year} B_M(t)dt$ is shown in Fig. 3 (solid line). The amount of the aerosol in the atmosphere during strong dust events appeared to be 25-30% which is in good agreement with the crude estimate made in the Introduction. Same calculations, but for the region in Europe (15^o W – 40^o E, 48^o N -51^0 N) are presented in Fig. 3 by the dashed line. The relative role of days with high AOT is somewhat larger (35-40%) but strong events still cannot be considered as the major part of aerosol loading.

4. Seasonal patterns of Aerosol Optical Thickness distribution

4.1 Seasonal dependence of aerosol appearance probability

First we determine seasons of different dust activity in the Mediterranean. We consider the AOT within the rectangular area between 15^oW - 40^o E, and 30^o N - 40^o N (Fig. 4, middle panel). Monthly averaged Aerosol Optical Thickness is integrated along the meridian for each given longitude λ. In order to diminish the effects of the background (the rectangle includes land areas, and even areas where the data on AOT are absent), the integrated monthly averaged AOT is normalized by its sum during a year:

$$A(t_i,\lambda) = \frac{\int_{30}^{40} AOT(t_i,\varphi,\lambda)d\varphi}{\sum_{i=1}^{12}\int_{30}^{40} AOT(t_i,\varphi,\lambda)d\varphi} \qquad (2)$$

where φ is the latitude, and t_i -month of a year.

The normalized quantity *A* characterizes the monthly probability of dust loading at the given longitude. The results are shown in the bottom panel (Fig. 4). The horizontal and vertical axes correspond to the longitude and months, respectively. The AOT occurrence *A* is color coded.

The dust activity region is displaced westward during the period from February till September in compliance with established Mediterranean dust seasonal variations

[*Moulin et al.,* 1998; *Israelevich et al*., 2002]. Vertical lines show approximate boundaries between three regions showing distinctly different AOT seasonal dependence -Eastern, Central and Western Mediterranean. The same boundaries are shown in the middle panel. For the whole Mediterranean region, three different seasons -I (March-May), II (June-July), and III (August September) can be defined. They are emphasized by horizontal lines. In the western sector, there is no clear difference between Seasons II and III, they are rather merged in one season in this region.

A similar analysis is performed for the region in Europe within 15^o W - 40^o E, 48^o N – 51^0 N which is also shown in the middle panel of Fig. 4. Noteworthy, the seasons of aerosol activity in this region of Europe are the same as in the Mediterranean, but the geographical distribution of the aerosol episodes is different. First of all, during the Season I, aerosols are observed in Europe in the whole range of longitudes, whereas the dust activity in the Western Mediterranean is low. Also, there are two separate maxima of aerosol activity (March and May) in the western part of the selected area (15^oW - 5^o E), especially above the ocean (15^oW - 5^0 W). These maxima correspond to the high activity of the Saharan sources in Bodele (~17^oE, 17^oN) (March) and El Djouf (~7W,20N) (May) regions (*Prospero et al*., 2002, *Israelevich et al*., 2002, *Koren et al*., 2006). If so, the dust in this region is transported over the Atlantic ocean as shown in the left panel of Fig. 1. Further eastward transport may also add to the observed AOT in the longitude range 5^o E – 40^o E. However, as it will be shown below, direct dust transport over the Mediterranean to this area is also possible.

During the Season II period, the aerosol activity occur predominantly in Central Europe (5^o E – 20^o E) thus indicating desert aerosol transport over the Central Mediterranean. In August-September (Season III), the AOT is highest in the eastern part of Europe (25^o E – 40^o E). These events may be of local origin, but taking into account the fact that during the same period dust activity increases in the Eastern Mediterranean the appearance of desert aerosols in Eastern Europe cannot be excluded.

4.2 Aerosol transport paths

Following *Israelevich et al*. [2002, 2003], the aerosol transport paths above the region of interest are obtained from the following properties of 10-year (2001 - 2010) average MODIS AOT distributions: positions of local maxima and the bands of the increased AOT. The enhanced AOT bands visualize the dust transport routes. Within the band, direction of propagation is from the region with high AOT to the region with lower AOT. We assume that near the North Africa coast desert dust is the major component of aerosol load (e.g. *Barnaba and Gobbi*, 2004). We investigate spatial and temporal variations of the 10-year mean AOT above the Mediterranean Sea and Europe, and more specifically over the area extending from 20^{o} N to 70^{o} N and from 30^{o} W to 50^{o} E. We consider the AOT as a measure of amount of aerosol in the air column. Therefore, the AOT integrated over certain area is the measure of the aerosol amount over the region.

Daily AOT distributions are averaged over the three periods denoted in Fig. 4. The produced seasonal distributions are given in the left panel of Fig. 5. Arrows in the right panel of Fig. 5 show the predominant transport of desert aerosol. In the Southern Mediterranean, the pattern is similar to that derived from TOMS aerosol index data [*Israelevich et al*., 2003]. During March-May, dust is transported predominantly eastward. The transport route over the Atlantic Ocean turning eastward to Europe is also visible. In June-July, aerosols from Sahara move northward and westward, whereas dust dynamics in the Eastern Mediterranean is determined by “Red Sea sources” on both the African and Arabian coasts of the Red Sea [*Prospero et al*., 2002; *Israelevich et al*., 2003]. General features remain the same in August-September with further displacement of activity westward.

In the Central Mediterranean, aerosol transport is predominantly northward during all three periods. In this region, dust transport to Europe is less significant in March-May, being the strongest during the June-July period. The predominant direction of dust transport is north-west-westward.

In Seasons II and III, AOT average distributions over Central Europe are similar. In August-October, a significant amount of aerosols is observed over Eastern Europe (55^o N, 25^o E-30^o E), (Fig. 5, bottom panel) whereas in June-July the average AOT is rather low. In Season III, the region of enhanced aerosol content is connected to dusty regions in both Central Europe and the Eastern Mediterranean. Basing only on AOT average distributions, it is impossible to conclude whether aerosols were transported from Central Europe, or dust was brought from Middle East sources through the Eastern Mediterranean, or both routes were valid for this season.

The local AOT maxima, denoted as A, B, C and D in Fig. 5, are noteworthy. Maximum A is located over North Italy, south of the Alps, and is observed almost around the whole year, except for January and December. Maximum B is observed south-east of the Pirenees, C -east of Sierra Nevada, and D -south of the Rila Mountains. The existence of these maxima might be a manifestation of desert dust transport over the Mediterranean to Europe. Indeed, if the dust carrying flow decelerates as it approaches the mountains, the dust concentration and AOT should increase. This can be expected for the Pyrenees (north-west directed dust transport), for Sierra Nevada (westward transport), for the Rila (northward transport), and for the Alps (also northward transport). This effect will be discussed in section 5.

Aerosol index (AI) [*Torres et al.*, 1998, 2007] can be considered as another measure of the aerosol amount in the air column. It is not as sensitive to surface albedo as MODIS AOT and is obtained (contrary to MODIS AOT) for the regions with high reflectance in Sahara desert. By definition, positive values of AI correspond to absorbing aerosols. As compared to MODIS AOT, aerosol index is relatively more sensitive to coarse mode particles and, because of Rayleigh scattering to high altitude aerosol layers. Therefore, is interesting to compare the pattern of transport paths derived from MODIS AOT (Fig. 5) with AI data. We apply the same procedure to OMI AI for the years (2004-2010) and consider the bands of enhanced average OMI AI as transport path. The results are shown in the right panels of Fig. 5. Along the transport paths, the AI decreases faster than MODIS AOT. In general, it is explained by the change of particle size distribution - over the Europe the ratio of coarse mode to fine mode drops as the relative role of anthropogenic aerosols becomes more significant. Above the Mediterranean, where OMI is high enough, the general pattern remains the same as in left panels (MODIS AOT distributions), with the same seasonal trend. However, the total absence of maxima in front of the mountains assumes that the aerosol layers producing these maxima are too low in order the presence can be revealed in UV.

Since the amount of aerosol transported during the dusty days is comparable with the background transport during relatively quiet periods, it is instructive to compare ”events” and ”background” transport paths.

All daily AOT data are separated in two groups. We define as a ”dusty event” the day when daily AOT, integrated over the Mediterranean region (0^o - 40^o E, 30^o N - 40^o N), was at least 20% larger than its 30-day average level. The first group includes all dusty days plus two days immediately following the dusty one. The latter is done in order not to miss the days when the aerosol cloud leaves the region of integration but still may exist. The rest of the days are included in the second group of non-dusty days.

Figure 6 shows the AOT distributions averaged over dusty (middle panels) and non-dusty (right panels) days, along with the distributions averaged over the whole seasons (left panels). Top panels correspond to the Season I, middle panels to the Season II, and lower panels -to Season III.

Analysis of Fig. 6 reveals that the transport routes for ”dusty” and ”non-dusty” days are similar with two exceptions. First, the transport in Eastern Mediterranean is different on dusty days and on non-dusty days in Season I. Strong dust events propagate along the African coast eastward, whereas this transport path disappears on the days low dust activity. The high dust loading is a consequence of the Sharav cyclone and the eastward dust path visualizes the motion of the cyclone [*Alpert and Ziv*, 1989; *Israelevich et al*., 2001]. Therefore, selecting days with high dust loading, we, in fact, select days with the Sharav cyclone and dust transport to Eastern Mediterranean. On non-dusty days (the second group), the Sharav cyclone is absent and there is no eastward transport.

Second, in Season III, Mediterranean dust events, i.e. the increased AOT over the Mediterranean (0^0 – 40^0 E, 30^o N – 40^o N), are accompanied by increased AOT in Eastern Europe (35^o - 45^o E, 52^o N -58^o N). On non-dusty days (the second group), aerosol activity in Eastern Europe also remains low. This is an argument in favor of possibility of Mediterranean dust tranport to Eastern Europe.

5. Aerosol Transport and Mountains

The local AOT should increase if the horizontal flow carrying aerosols is decelerated in front of mountains. As it was mentioned at the end of Section 3, this mechanism might be responsible for local maxima of AOT near the Alps, Pyrenees, Sierra Nevada and Rila shown in Fig. 5. On the other hand, these maxima may be produced by local aerosol sources like industrial pollution, soil erosion etc. Let us consider the enhancement of AOT in front of the Alps above the Po valley (marked by A in Fig. 5). The Season I MODIS AOT distribution fits very well the mountain relief of the Alps as it is shown in Fig. 7 laying AOT over the satellite image of Northern Italy.

Being an industrial region, Po valley is the place of strong anthropogenic industrial pollution [*Barkan et al*.,2005; *Barnaba and Gobbi,* 2004]. There are also no doubts that significant amounts of desert dust ocassionally appear in this region. Dust from Sahara plays the essential role in the neutralization precipitation [*Pieri et al*., 2010].

Health effects of desert dust presence in Po valley were also observed [*Sajani et al*., 2010].

Moreover, deceleration of the northward dust carrying flow from the Central Mediterranean near the Alps may also create a kind of 'trap' resulting in an increase of dust 244 concentration and AOT maximum in this region, as observed by MODIS instrument (Fig. 5). For example, aerosol was trapped in the Po valley on October 13, 2001, and the results of aerosol mask application to the region above the Adriatic sea adjacent to Po valley show that the aerosol in the 'trap' is mainly desert dust [*Barnaba and Gobbi,* 2004, see Fig. 5 therein].

Figure 8 shows monthly averaged AOT integrated over the region 44^{o} – 46^{o} N, 7^{o} - 14^{o} E (North Italy). The largest values are observed in the April-June period, which is typical for the Central Mediterranean as it can be expected for desert dust transport through the Mediterranean to Europe.

In order to verify this assumption, we consider in the region 7^{0} E -15^{o} E, 30^{o} N - 55^{o} N (Fig. 9, top panel) the daily AOT integrated over the longitude:

$$C(t_i,\varphi) = \int_7^{15} AOT(t_i,\varphi,\lambda)d\lambda \qquad (3)$$

The results of $C(t, \varphi)$ calculations for the year 2008 are presented in Fig. 9 (middle panel). The bottom panel shows a part of the middle panel in increased scale.

Being rather short (~2 days), dust events are distributed continuously along wide range of latitudes. A clear increase of AOT can be seen near the latitude of the southern Alps denoted by the arrow, as it should be for the decelerated northward flow. Also, there are no enhancements of AOT above the Po valley which are not extended southward. Sources of industrial pollution operate rather continuously. Therefore, if the AOT maxima are produced by pollution, one can expect that they should be prominent, when the aerosol transport with air masses is weak or absent, and they should decrease in cases, when the aerosol is distributed over larger areas due to the transport motion. Figure 9 demonstrates quite opposite behavior. The aerosol amount above the Po valley usually increases for the events with latitude spread. Thus, we conclude that the effect of flow deceleration by mountain relief, causing AOT increase, indeed takes place.

6. Conclusion

Our analysis of monthly averaged AOT distributions over Europe for the period 2001 - 2010 revealed three seasons of aerosol activity above the continent. They coincide with three distinct seasons of desert dust activity in the Mediterranean region, namely, March-May, June-July and August-September. Over Western Europe (15^{o} W-5^{o} E), AOT is the highest in spring, contrary to the Western Mediterranean where the highest AOT is observed in autumn. In spring, the predominant dust transport route from Saharan sources to Western Europe is a westward motion of dust plumes by trade winds, with subsequent turn northward and then back to the East. Over Central Europe (5^{o} E – 25^{o} E) the aerosol activity has two maxima, in the spring and summer seasons, whereas over Eastern Europe (25^{o}- 40^{o}E) AOT is highest in spring and autumn. The dust is brought to these sectors from the Eastern Mediterranean by air masses moving northward.

The existence of aerosol transport routes toward Europe is manifested by the appearance of localized regions of increased average AOT on the Mediterranean side of mountain ranges (the Alps, Rila, Pyrenees, Sierra Nevada). In those regions, AOT increases due to deceleration of the horizontal flow carrying aerosols in front of the mountains.

Acknowledgments. MODIS-Terra and MODIS-Aqua daily data of aerosol optical thickness data at 550 nm were obtained from NASA's MODIS Data Processing System (MODAPS) website (http://ladsweb.nascom.nasa.gov/data/search.html). Daily data of OMI Aerosol Index were obtained Giovanni online data system, developed and maintained by the NASA GES DISC. We acknowledge the mission scientists and Principal Investigators who provided the data used in this research effort.

References

Alpert, P., and B. Ziv, The Sharav Cyclone - Observation and some Theoretical Considerations, J. Geophys. Res., 94, 18,495 – 18,514, 1989.

Barkan, J., H. Kutiel, and P. Alpert (2004a), Climatology of dust sources in North Africa and the Arabian Penninsula based on TOMS data, Indoor and Built Environment, 13, 407–419, doi: 10.1177/1420326X04046935.

Barkan, J., H. Kutiel, P. Alpert, and P. Kishcha (2004), Synoptics of dust intrusion days from the African continent into the Atlantic Ocean, J. Geophys. Res, 109, D08201, doi:10.1029/2003JD004416.

Barkan, J., P. Alpert, H. Kutiel, and P. Kishcha (2005), Synoptics of dust transportation days from Africa toward Italy and central Europe, J. Geophys. Res, 110, D07208, doi:10.1029/2004JD005222.

Barkan, J., and P. Alpert (2008), Synoptic patterns associated with dusty and non-dusty seasons in the Sahara, *Theor. Appl. Climatology*, *94*, 153–162, doi: 10.1007/s00704-007- 0354-9.

Barnaba, F. and G. P. Gobbi (2004), Aerosol seasonal variability over the Mediterranean region and relative impact of maritime, continental and Saharan dust particles over the basin from MODIS data in the year 2001, Atmos. Chem. Phys., 4, 2367–2391.

Engelstaedter, S., and R. Washington (2007), Atmospheric controls on the annual cycle of North African dust, J. Geophys. Res., 112, D03103, doi:10.1029/2006JD007195.

Engelstaedter, S., I. Tegen, and R. Washington (2006), North African dust emissions and transport, Earth Sci. Rev., 79, 73-100, doi:10.1016/j.earscirev.2006.06.004.

Escudero, M., S. Castillo, X. Querol, A. Avila, M. Alarcon, M. M. Viana, A. Alastuey, E. Cuevas, S. Rodriguez (2005), Wet and dry African dust episodes over eastern Spain, J. Geophys. Res, 110, D18S08, doi:10.1029/2004JD004731.

Ganor, E. (1994), The frequency of Saharan dust episodes over Tel Aviv, Israel, Atmos. Environ., 28, 2867-2871, doi:10.1016/1352-2310(94) 90087-6.

Ganor, E., Y. Deutsch, and H.A. Foner (2000), Mineralogical composition and sources of airborne settling particles on Lake Kinneret (the sea of Galilee) in Israel, Water, Air, and Soil Pollution, 118, 245–262.

Ganor, E., I. Osetinsky, A. Stupp, P. Alpert (2010), Increasing trend of African 315 dust, over 49 years,in the eastern Mediterranean, J. Geophys. Res, 115, D07201, doi:10.1029/2009JD012500.

Gerasopoulos, E., V. Amiridis, S. Kazadzis, P. Kokkalis, K. Eleftheratos, M. O. Andreae, T. W. Andreae, H. El-Askary and C. S. Zerefos (2011) Three-year ground based measurements of aerosol optical depth over the Eastern Mediterranean: the urban environment of Athens, Atmos. Chem. Phys., 11, 2145–2159, doi:10.5194/acp-11-2145-2011.

Goudie, A. S., N. J. Middleton (2001), Saharan dust storms: Nature and consequences, Earth Sci. Rev., 56, 179-204, doi:10.1016/S0012-8252(01)00067-8.

Gkikas, A., N. Hatzianastassiou, and N. Mihalopoulos (2009), Aerosol events in the broader Mediterranen basin based on 7-year (2000 2007) MODIS C005 data, Ann. Geophys., 27, 3509–3522.

Israelevich, P. L., Z. Levin, J. H. Joseph, and E. Ganor (2002), Desert aerosol transport in the Mediterranean region as inferred from the TOMS aerosol index, J. Geophys. Res, 107 (D21), 4572, doi:10.1029/2001JD002011.

Israelevich, P.L., E. Ganor, Z. Levin, and J.H. Joseph (2003), Annual variations of physical properties of desert dust over Israel, J. Geophys. Res, 108 (D13), 4381, doi 10.1029/2002JD003163.

Jilbert, T., G.-J. Reichart, B. Aeschlimann, D. G¨unther, W. Boer and G. de Lange (2010), Climate-controlled multidecadal variability in North African dust transport to the Mediterranean, Geology, 38, 19–22, doi: 10.1130/G25287.1.

Kalivitis, N., E. Gerasopoulos, M. Vrekoussis, G. Kouvarakis, N. Kubilay, N. Hatzianastassiou, I. Vardavas, and N. Mihalopoulos (2007), Dust transport over the eastern Mediterranean derived from Total Ozone Mapping Spectrometer, Aerosol Robotic Network, and surface measurements, J. Geophys. Res., 112, D03202, doi:10.1029/2006JD007510.

Kishcha, P., S. Nickovic, E. Ganor, L. Kordova, and A. Alpert (2008), Saharan dust over the Eastern Mediterranean: Model sensitivity, in Air pollution modeling and its applications XIX, Chapter 4.2, Springer, 358–366.

Koren, I, Y. J. Kaufman, R. Washington, M. C. Todd, Y. Rudich, J. Vanderlei Martins, and D. Rosenfeld (2006), The Bod´el´e depression: a single spot in the Sahara that provides most of the mineral dust to the Amazon forest, Environ. Res. Lett., **1** 014005 , doi:10.1088/1748-9326/1/1/014005.

Koltay, E., I. Borb´ely-Kiss, Zs. Kert´esz, A. Z. Kiss and Gy. Szab´o (2006), Assignment of Saharan dust sources to episodes in Hungarian atmosphere by PIXE and TOMS observations, J. Radioanal. Nucl. Chem., 267, 449–459.

Levin, Z., E. Ganor, and V. Gladstein (1996), The effects of desert particles coated with sulfate on rain formation in the eastern Mediterranean, J. Appl. Meteorol., 35, 1511-1523.

Littmann, T., and J. Steinrucke (1989), Atmospheric Boundary Conditions of Re-cent Saharan Dust Influx into Central Europe, GeoJournal 18, 399–406, doi:

10.1007/BF00772694.

Moulin, C., F. Guillard, F. Dulac, and C.E. Lambert (1997), Long-term daily monitoring of Saharan dust load over ocean using Meteosat ISCCP-B2 data: 1. Methodology and preliminary results for 19831994 in the Mediterranean, J. Geophys. Res, 102 (D14), 16947-16958, doi:10.1029/96JD02620.

Moulin, C., C.E. Lambert, U. Dayan, V. Masson, M. Ramonet, P. Bousquet, M. Legrand, Y.J. Balkanski, W. Guelle, B. Marticorena, G. Bergametti, and F. Dulac (1998), Satellite climatology of African dust transport in the Mediterranean atmosphere, J. Geophys. Res, 103 (D11), 13137–13144.

Papayannis, A., V. Amiridis, L. Mona, G. Tsaknakis, D. Balis, J. Bosenberg, A. Chaikovski, F. De Tomasi, I. Grigorov, I. Mattis, V. Mitev, D. Muller, S. Nickovic, C. Perez, A. Pietruczuk, G. Pisani, F. Ravetta, V. Rizi, M. Sicard, T. Trickl, M. Wiegner, M. Gerding, R. E. Mamouri, G. DAmico, and G. Pappalardo (2008), Systematic lidar observations of Saharan dust over Europe in the frame of EARLINET (20002002), J. Geophys. Res, 113, D10204, doi:10.1029/2007JD009028.

Perez, L., A. Tobias, X. Querol, N. K¨unzli, J. Pey, A. Alastuey, M. Viana, N. Valero, M. Gonz´alez-Cabr´e and J. Sunyer (2008),. Coarse particles from Saharan dust and daily mortality, Epidemiology, 19,:800e7, doi: 10.1097/EDE.0b013e31818131cf

Pieri, L., P. Matzneller, N. Gaspari, I. Marotti, G. Dinelli and P. Rossi (2010), Bulk Atmospheric Deposition in the Southern Po Valley (Northern Italy), Water Air Soil Pollut., 210, 155–169, doi 10.1007/s11270-009-0238-y.

Prospero, J.M. (1999), Long-term measurements of the transport of African mineral dust to the southeastern United States: implications for regional air quality, J. Geophys. Res, 104 (D13), 15917–15927.

Prospero, J.M., P. Ginoux, O. Torres, S. E. Nicholson, and T. E. Gill, Environmental characterization of global sou7rces of atmospheric soil dust identified with the nimbus 7 total ozone mapping spectrometer (TOMS) absorbing aerosol product, *Rev. Geophys.*, *40*(1), 1002, doi:10.1029/2000RG000095, 2002.

Querol, X., A. Alastuey, J. Pey, N. Perez, M. Escudero, S. Castillo, A. Cristobal, M. Pallares, A. Gonzalez, S. Jimenez, N. Alonso, S. Alonso-Perez, E. Cuevas, and J. de 376 la Rosa (2009), African dust influence on ambient PM levels in South-Western Europe (Spain and Portugal): A quantitative approach to support implementation of Air Quality Directives. IOP Conf. Ser.: Earth Environ. Sci., 7, 012018, doi: 10.1088/1755-1307/7/1/012018.

Remer, L. A., Y. J. Kaufman, D. Tanre, S. Mattoo, D. A. Chu, J. V. Martins, R-R. Li, C. Ichoku, R. C. Levy, R. G. Kleidman, T. F. Eck, E. Vermote, and B. N. Holben (2005), The MODIS Aerosol Algorithm, Products and Validation, J. Atmosph. Sci., 62, 947-973.

Rosenfeld, D., Y. Rudich, and R. Lahav (2001), Desert dust suppressing precipitation: A possible desertification feedback loop, Proc. Natl. Acad. Sci. U. S. A., 98, 5975-5980.

Sajani, S. Z., R. Miglio, P. Bonasoni, P. Cristofanelli, A. Marinoni, C. Sartini, C. A. Goldoni, G. De Girolamo and P. Lauriola (2010) Saharan dust and daily mortality in Emilia-Romagna (Italy), Occup. Environ. Med., doi:10.1136/oem.2010.058156.

Torres, O., P. K. Bhartia, J. R. Herman, Z. Ahmad, and J. Gleason (1998), Derivation of aerosol properties from satellite measurements of backscattered ultraviolet radiation: Theoretical basis, J. Geophys. Res., 103(D14), 17,099–17,110.

Torres, O., A. Tanskanen, B. Veihelmann, C. Ahn, R. Braak, P. K. Bhartia, P. Veefkind, and P. Levelt (2007), Aerosols and surface UV products from Ozone Monitoring Instrument observations: An overview, J. Geophys. Res., 112, D24S47, doi:10.1029/2007JD008809.

Wurzler, S., T. G. Reisin, and Z. Levin (2000), Modification of mineral dust particles by cloud processing and subsequent effects on drop size distributions, *J. Geophys. Res*, *105* (D4), 4501-4512.

Yin, Y., S. Wurzler, Z. Levin, and T. Reisin (2002), Interactions of mineral dust particles and clouds: Effects on precipitation and cloud optical properties, J. Geophys. Res, 107 (D23), 4724, doi:10.1029/2001JD001544.

List of Figures

Figure 1. Two transport paths for desert dust from North Africa to Western Europe. Atlantic path (left top panel) and Mediterranean path (right top panel). Lower panels show distribution of TOMS aerosol index corresponding to Atlantic path (March 05, 1997, left) and Mediterranean path (October 12, 2001, right).

Figure 2. Time dependence of the MODIS AOT integrated over the Mediterranean region BM (t) (thick line) and its lower envelope bM (t) (thin line).

Figure 3. The ratio of background to total aerosol amount for the period 2001-2010. Solid line - above Mediterranean, dashed line - above Europe.

Figure 4. Longitudinal and temporal dependence of the MODIS Aerosol Optical Thickness above two regions denoted in the middle panel (see text for explanation). Vertical lines show approximate boundaries between the regions showing distinctly different AOT seasonal dependence Eastern, Central and Western Mediterranean in the lower panel and Ocean, West, Central a nd East Europe in the top panel. Three different seasons of aerosol activity I (Spring), II (Middle Summer), and III (Summer-Autumn) are emphasized by horizontal lines in both panels.

Figure 5. (Left panels) MODIS Aerosol Optical Thickness distributions averaged for three seasons: (top) March-May, (center) June-July, (bottom) August-September. Cartoons in the middle panels denote corresponding aerosol transport paths. Right panels show the OMI Aerosol Index distributions averaged for the same periods.

Figure 6. MODIS AOT distributions averaged over dusty days (middle panels) and non-dusty days (right panels), along with distributions averaged over the whole seasons (left panels). Top panels correspond to the Season I, middle panels to the Season II, and lower panels to Season III.

Figure 7. Spring MODIS AOT distribution superimposed on the satellite image of South Europe. Only regions with AOT larger than 0.25 are shown.

Figure 8. The average seasonal variation of MODIS AOT in North Italy.

Figure 9. Dependence on time and latitude daily MODIS AOT integrated over longitude inside the region 7^o E - 15^o E, 30^o N - 55^o N (top panel). Middle panel - data for the year 2008, bottom panel -enhanced scale for August 1 November 15, 2008. Arrows denote the latitude of southern Alps' spurs.

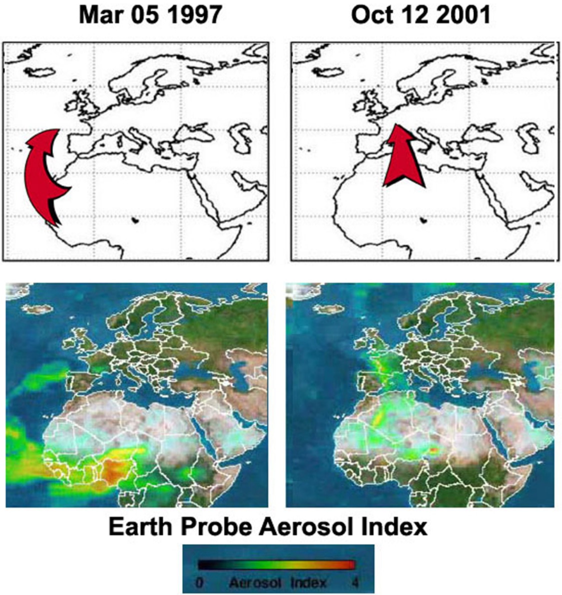
Mar 05 1997
Oct 12 2001
Earth Probe Aerosol Index
0
Aerosol Index
4

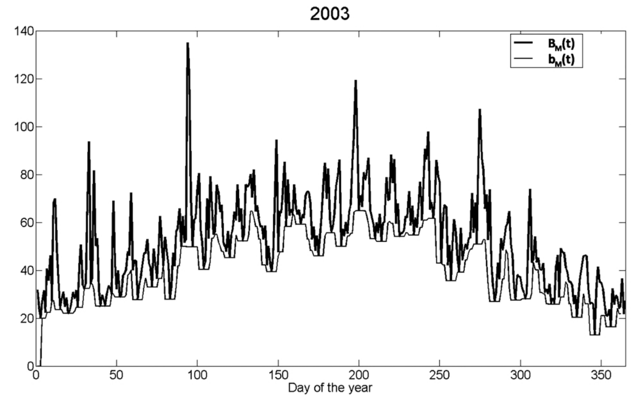

2003
140
120
100
80
60
40
20
0
0
50
100
150
200
250
300
350
Day of the year
B_M(t)
b_M(t)

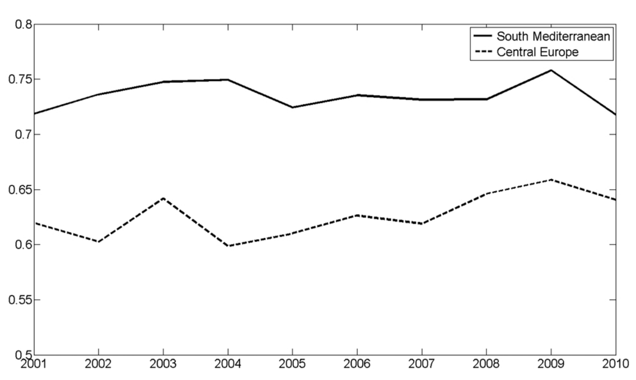

0.8
0.75
0.7
0.65
0.6
0.55
0.5
2001
2002
2003
2004
2005
2006
2007
2008
2009
2010
South Mediterranean
Central Europe

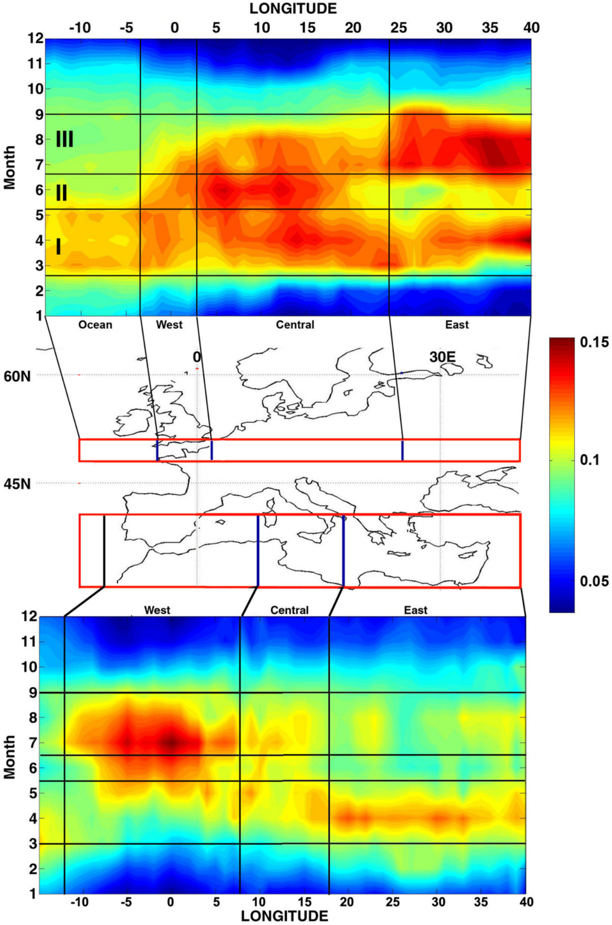

LONGITUDE
Month
III
II
I
Ocean
West
Central
East
0
30E
60N
45N
0.15
0.1
0.05
West
Central
East
Month
LONGITUDE

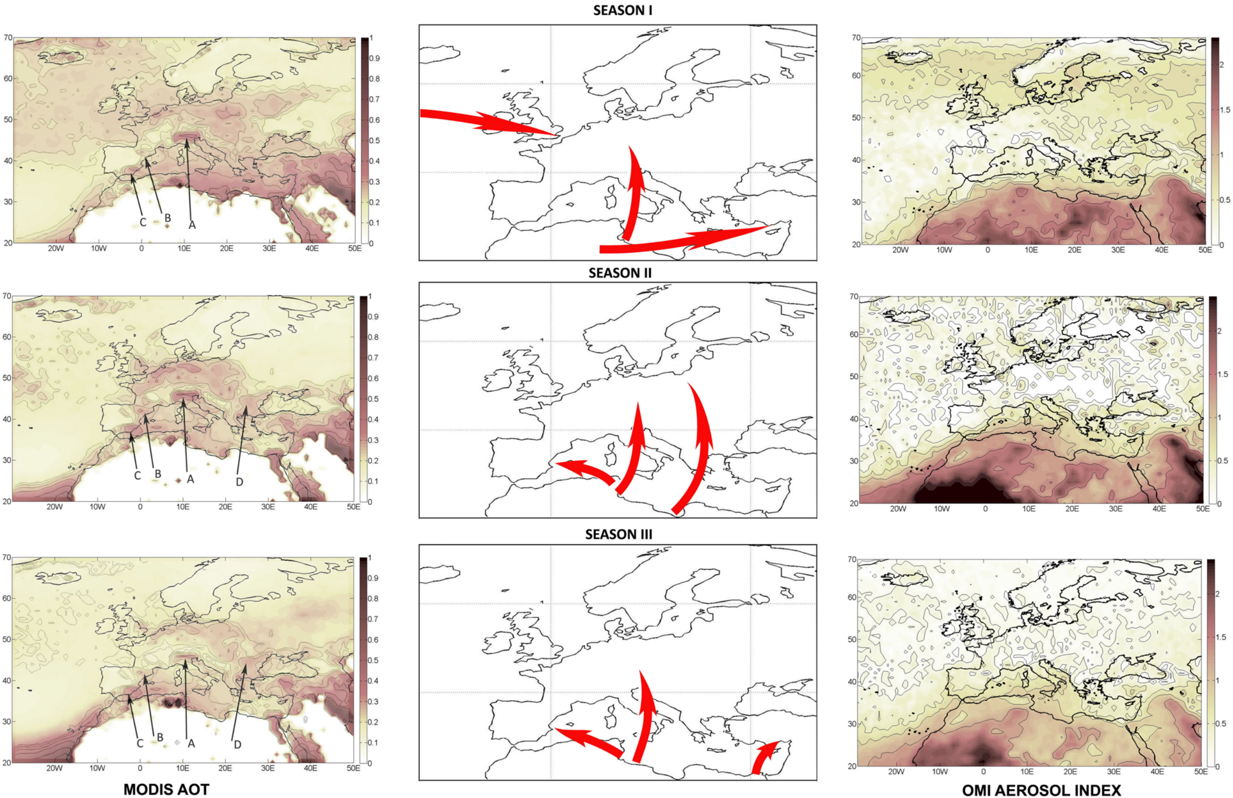

SEASON I
SEASON II
SEASON III
A
B
C
D
70
60
50
40
30
20
20W
10W
0
10E
20E
30E
40E
50E
0
0.1
0.2
0.3
0.4
0.5
0.6
0.7
0.8
0.9
1
0.5
1.5
2
MODIS AOT
OMI AEROSOL INDEX

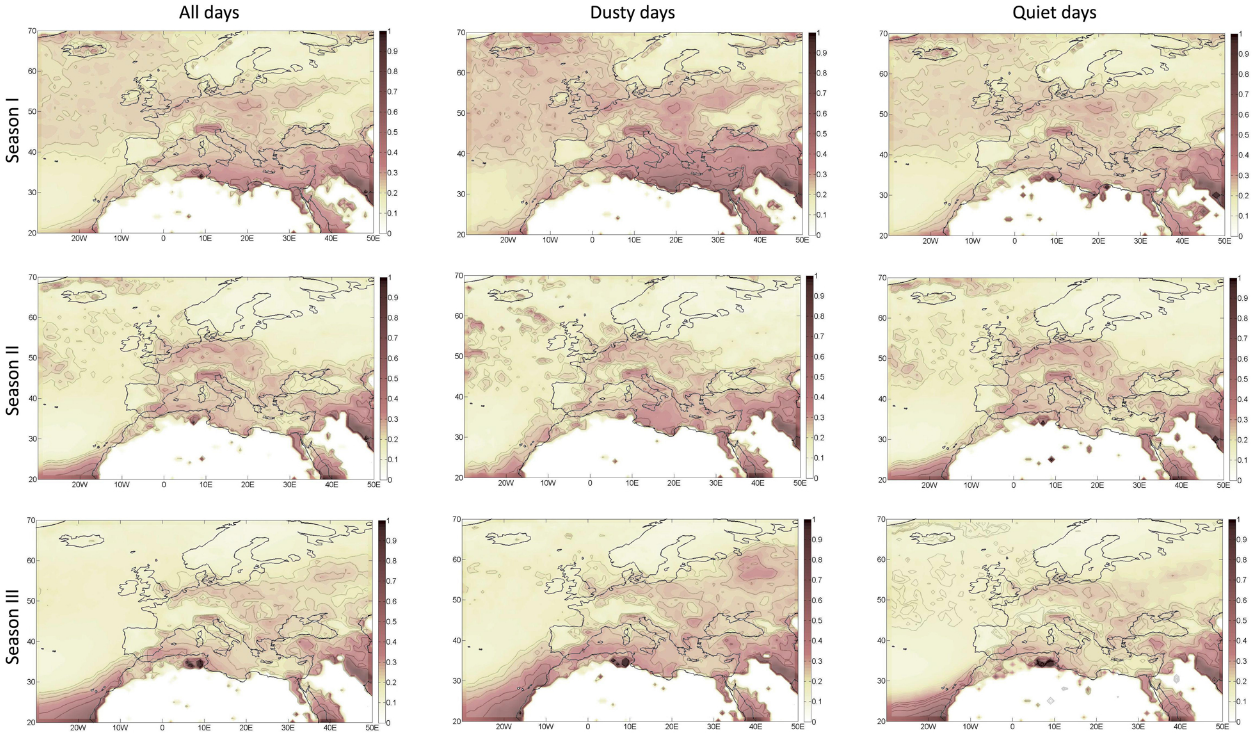
All days
Dusty days
Quiet days
Season I
Season II
Season III

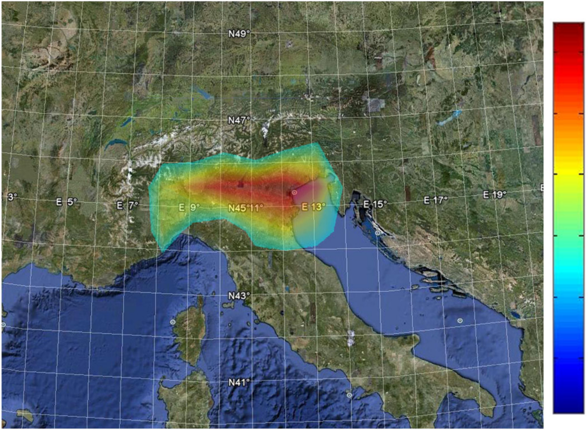

N49°
N47°
3°
E 5°
E 7°
E 9°
N45°11°
E 13°
E 15°
E 17°
E 19°
N43°
N41°
0.6
0.5
0.4
0.3
0.2
0.1

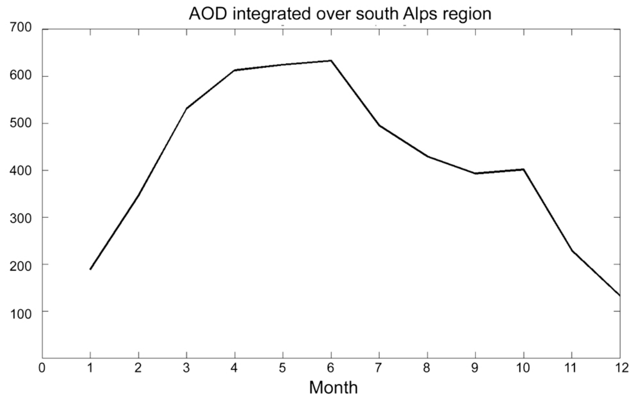
AOD integrated over south Alps region
700
600
500
400
300
200
100
0
1
2
3
4
5
6
7
8
9
10
11
12
Month

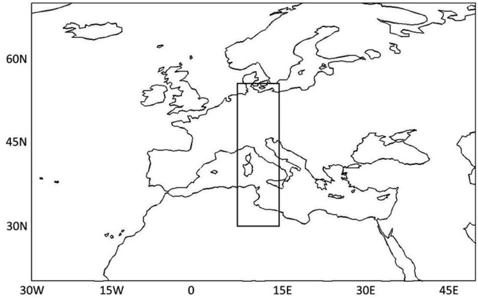
60N
45N
30N
30W
15W
0
15E
30E
45E

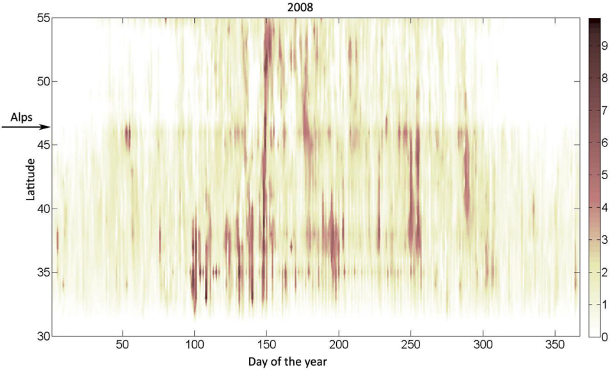
2008
Alps
Latitude
Day of the year
55
50
45
40
35
30
50
100
150
200
250
300
350
0
1
2
3
4
5
6
7
8
9

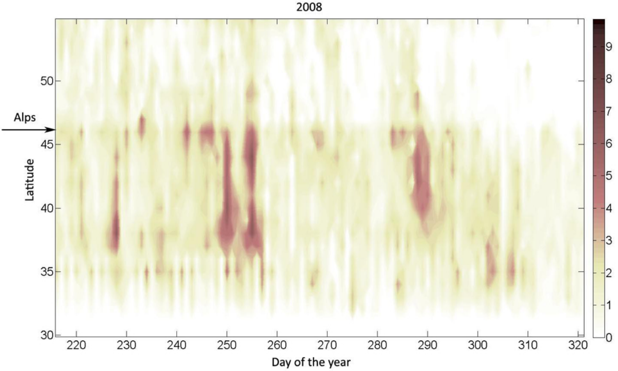
2008
Alps
Latitude
Day of the year
50
45
40
35
30
220
230
240
250
260
270
280
290
300
310
320
0
1
2
3
4
5
6
7
8
9